



Growth and characterization of pure and metals-doped organic nonlinear optical single crystal: L-alanine alaninium nitrate (LAAN)

G. Krishnamoorthi¹ and R. Uvarani^{1,*}

¹PG and Research Department of Physics, Thiruvalluvar Government Arts College, Rasipuram, Tamil Nadu 637401, India

Received: 7 October 2020

Accepted: 16 December 2020

Published online:
6 January 2021

© The Author(s), under exclusive licence to Springer Science+Business Media, LLC part of Springer Nature 2021

ABSTRACT

The pure and metal ion (Cu^{2+} , Zn^{2+} and Mg^{2+})-doped LAAN single crystal was developed by slow evaporation technique under ambient temperature. Cell parameters of the grown crystal were identified using single crystal X-ray diffraction analysis and found that the material crystallizes in orthorhombic crystal system with space group of P21. The presence of functional groups and the spectral properties were assessed by FTIR analysis. Transmittance spectrum reveals that the crystal has a low UV cut-off of 360 nm and has a good transmittance in the entire visible region. The band gap energy of LAAN and doped (Zn, Cu and Mg) LAAN crystals were estimated to be 3.38, 3.22, 2.75, and 3.13 eV by Tauc plot. Prevention of the recombination process of electron-hole pair was also confirmed by photoluminescence spectra analysis. The dielectric constant of pure crystal was found to be less than that of doped crystals. The AC conductivity was found to increase after doping and with the increase in temperature. Second harmonic generation efficiency of the grown crystal has been measured by Kurtz and Perry technique and it was found that Cu-doped LAAN is 3.2 times higher than that of KDP and 2.1, 1.5, and 1.8 times more prominent than pure, Zn, and Mg-doped LAAN crystals, respectively.

1 Introduction

In recent years, nonlinear optical (NLO) materials have attracted considerable attention due to their applications in laser technology, optical communications, optical switching, data storage, optical mixing, and electro-optic applications. The development of organic materials suitable for nonlinear optical devices is of interest because of high nonlinearity when

compared to that of conventional inorganic materials. A considerable interest has been shown recently in studying the effect of impurities (both inorganic and organic) on the nucleation, growth, and physical properties of some hydrogen bonded crystals like potassium dihydrogen phosphate (KDP), ammonium dihydrogen phosphate (ADP), magnesium sulfate heptahydrate (MSH), ammonium oxalate monohydrate (AOM), and zinc tris (thiourea) sulfate (ZTS)

Address correspondence to E-mail: gkmpysics@gmail.com

[1–9]. The presence of impurity molecules even at lower concentrations in the parent solute may have considerable effect on growth kinetics and other properties.

Several interesting results have already been reported on several properties of doped KDP [1–3], AOM [4, 5], MSH [6, 7], and ZTS [8, 9] crystals. Some reports are also available on doped ADP single crystals [1, 10]. Ananda Kumari and Chandramani [11] have found that the KDP crystals containing alkali halides such as potassium chloride (KCl)/sodium chloride (NaCl)/potassium bromide (KBr)/sodium bromide (NaBr)/potassium iodide (KI)/sodium iodide (NaI) show appreciable increase in second harmonic generation (SHG) efficiency compared to pure KDP crystals. Deepa et al. [12], have showed that the alkali halide (NaCl/NaBr) addition reduces the DC conductivity of KDP single crystals. Anne Assencia and Mahadevan [10] have observed the DC conductivity of ADP single crystal increases with the increase in impurity (urea/thiourea) concentration. Mahadevan [13] has found that the DC conductivity does not vary systematically with impurity concentration in the case of KCl-added MSH single crystals. However, the conductivity is larger for impurity-added crystals than the pure crystals. Meena and Mahadevan [1] have reported that L-arginine ($C_6H_{14}N_4O_2$) addition leads to reduction of electrical parameters of KDP and ADP single crystals. Considering the above, it can be understood that impurity (various types) addition to L-alanine alaninium nitrate (LAAN) is expected to make it a more interesting material. Therefore, understanding the effect of different kinds of impurities on the physical properties of this material needs more investigations. The L-alanine alaninium nitrate (LAAN) belongs to the family of organic nonlinear optical material and is grown from its aqueous solution by slow evaporation technique at room temperature. The characterizations of the grown single crystals were investigated by many researchers [14–19]. The L-alanine alaninium nitrate (LAAN) was first crystallized by Manuela Ramos Silva [20], which belongs to the monoclinic crystal system with space group P21 with cell parameters $a = 7.8578$ (5) Å, $b = 5.4516$ (6) Å, $c = 12.8276$ (7) Å, and $\beta = 94.73$ (4)°. We report the optical, dielectric, electrical, and NLO properties of divalent metal particles (Cu^{2+} , Zn^{2+} and Mg^{2+})-doped LAAN single crystals grown by slow evaporation method. To date, there is no report about

metal-doped LAAN single crystals and their physical and chemical properties. The characterization results suggest that Cu-doped LAAN single crystal show outstanding dielectric, electrical, and NLO properties than other dopants.

2 Experimental

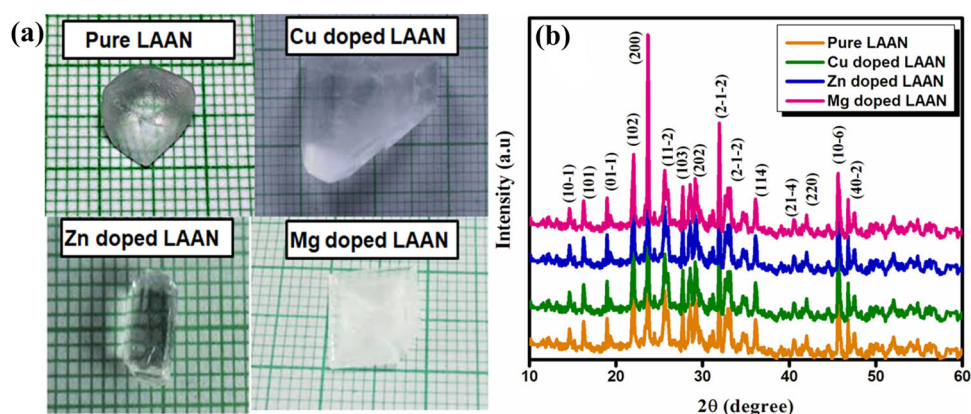
2.1 Crystal growth

The single crystal of LAAN was synthesized from L-alanine and nitric acid taken in the stoichiometric ratio of 2:1. Ived in double-distilled water. In order to synthesize the doped LAAN, the calculated amount of $CuCl_2$, $ZnCl_2$ and $MgCl_2$ additives were added to the solution of LAAN separately. The solutions of pure and doped LAAN were prepared separately and stirred well using a magnetic stirrer for about 2 h. The solutions were heated at 50 °C until the synthesized salts of pure and doped LAAN were obtained. The synthesized LAAN was purified by repeated recrystallization process before growth to improve the purity of the material. The high-purity material (purified material) yields good quality crystals. The solution of recrystallized LAAN was prepared at 40 °C using water as a solvent. The bulk single crystals of L-alanine alaninium nitrate were harvested after 2 weeks. The photographs of pure and doped LAAN single crystals are shown in Fig. 1a.

2.2 Characterization techniques

The cell parameters of the grown crystal were determined from the powder X-ray diffraction pattern using standard software. The optical transmission spectrum was recorded in the range 200–1100 nm using Lambda 35 UV-Vis-NIR spectrometer for a crystal of thickness 1 mm. The microhardness of the crystal was measured using a microhardness tester (HMV-2) fitted with a Vickers diamond pyramidal indenter and attached with an optical microscope. Dielectric measurements were carried out using HIOKI 3532–50 LCR meter in the frequency range 100 kHz–2 MHz. The coordination of L-alanine with nitric acid was confirmed by FTIR studies using BRUKER 66 V FT-IT spectrometer in the range 4000–400 cm^{-1} following KBr pellet technique. The photoluminescence spectrum was

Fig. 1 **a** Photograph of grown crystals; **b** X-ray diffraction pattern of pure and doped LAAN crystals



recorded for LAAN single crystal using Perkin Elmer LS 55 luminescence spectrometer. The excitation wavelength used for the present study is 390 nm. Dielectric studies were carried out on (010) faces of the grown crystals using Hioki 3532-50 LCR Hitester. Microhardness measurements were carried out using Shimadzu tester. Second harmonic generation (SHG) of the samples was measured by Kurtz powder method. A Q-switched Nd:YAG laser beam of wavelength 1064 nm was used within an input energy of 5.02 mJ/pulse and the pulse width of 8 ns, with the depletion rate being 10 Hz. The SHG radiation of 532 nm (green light) emitted was collected by a photomultiplier tube (PMT-Philips Photonics model 8563) and the optical signal incident on the PMT was converted into voltage output at the CRO (Tektonic-TDS 3052).

3 Result and discussions

3.1 ICP and XRD analysis

The collected grown doped LAAN single crystals were converted to powder format and the powder was tested to the presence of dopant material percentage value analyzed by ICP technique. The doped LAAN crystal fine powder 10 mg was taken and mixed with 50 mL D.I water and tested to ICP measurement and the result confirms that the doped material presents at 3–5%. The sum of dopant solidified into the doped precious stone is less than the concentration of the dopant inside the comparing arrangement. Figure 1b shows the XRD results of bare and doped LAAN single crystals. These results include crystallographic order and structural perfection of grown crystals. The lattice parameter of both

crystals like $a = 7.851 \text{ \AA}$, $b = 5.441 \text{ \AA}$, $c = 12.806 \text{ \AA}$, $\beta = 94.75^\circ$, and volume of $V = 547 \text{ \AA}^3$ belong to space group P21. The presence of all units of crystal values is confirmed by already reported works [21]. The comparison of bare and doped LAAN crystal lattice parameters and volume are summarized in Table 1. The dopant material does not influence of crystal structure of LAAN. The presence of dopants in LAAN crystal may produce lattice strain which leads to change in unit cell parameters of the doped samples.

3.2 FTIR analysis

The FTIR spectral analysis of pure and doped LAAN crystals was carried out in the middle IR region between 400 and 4000 cm^{-1} to analyze the presence of functional groups in the crystals. Figure 2 shows the Fourier transform infrared spectrums of pure LAAN crystal. In the higher energy region, there is a broad intense band due to N–H stretch of NH^{3+} . There is a fine structure in the lower energy region of the band due to hydrogen bonding of NH^{3+} with COO^- in the crystal lattice for pure LAAN. The observed bands due to the fundamental vibration are in good agreement with the available literature data [22–24]. The sharp intense peaks which were

Table 1 Unit cell parameters of pure and doped LAAN crystals

Crystals	a (Å)	b (Å)	c (Å)	β (°)	Volume Å ³
Pure LAAN	7.851	5.441	12.806	94.05	544.81
Cu-doped LAAN	7.867	5.455	12.889	95.31	553.12
Zn-doped LAAN	7.854	5.408	12.742	94.15	541.21
Mg-doped LAAN	7.835	5.434	12.809	94.28	545.34

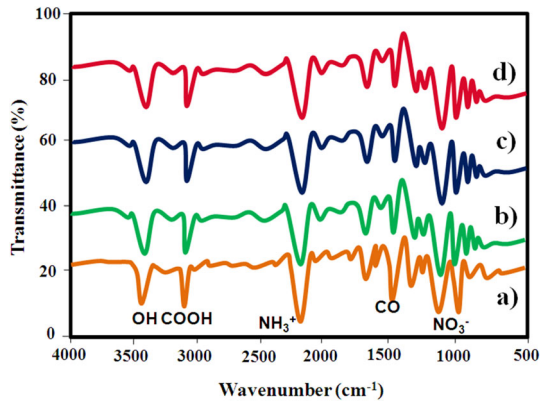


Fig. 2 FTIR spectra of **a** pure LAAN **b** Cu-doped LAAN; **c** Zn-doped LAAN; and **d** Mg-doped LAAN

observed in the range $2110.19\text{--}2112.12\text{ cm}^{-1}$ were assigned to the hydrogen bonding of NH_3^+ and COOH group. The bending modes of CH_3 are resolved in the region $1359.86\text{--}1361.79\text{ cm}^{-1}$ and $1503.38\text{--}1510.31\text{ cm}^{-1}$. The peaks at 1411.94 cm^{-1} are due to C–O stretch and the O–H bend of COOH group observed at $1232.55\text{--}1234.48\text{ cm}^{-1}$. From the IR spectrums, it is clear that the COO^- of pure and doped LAAN are protonated by nitric acid. The comparison of IR spectrums of pure and doped LAAN show slight shift in absorption bands which may be due to presence of doping. The vibration values of bare and doped LAAN single crystal are depicted in Table 2.

3.3 UV–Vis spectral analysis

The UV–VIS–NIR spectrum gives information about the structure of the molecule since the absorption of UV and visible light involves the promotion of electron and orbitals from the ground state to higher energy states. The UV–Vis spectrum of pure and doped LAAN crystals was recorded using Perkin–Elmer UV–Vis spectrophotometer in the range of

250–900 nm. The transmission spectra are very important for any NLO material because a NLO material can be of practical use only if it has a wide transparency window. The UV–Vis transmission was carried out by bare and doped LAAN crystals and the resultant plot is shown in Fig. 3a. The percentages of transmission in doped samples were found to be more when compared to the pure LAAN. From the UV spectral study, it can be concluded that both pure and doped LAAN crystals have good transmission in UV as well as in visible region which is an added advantage for the crystals to be used in optoelectronic applications. Transmittance spectrum reveals that the crystal has a low UV cut-off of 360 nm for pure LAAN, after incorporating the metal ions the band is shifted toward higher wavelength side. A considerable red shift is due to the decreasing the optical band gap energy of the crystals. The band gap energy of LAAN and doped (Zn, Cu and Mg) LAAN crystals were estimated to be 3.38, 3.22, 2.75, and 3.13 eV by Tauc plot (Fig. 3b) [25].

3.4 Photoluminescence spectral analysis

The instrument of Photoluminescence spectra was handled by 5 mW Ar^+ ion laser operated at 490 nm region and power density as 0.125 Wcm^{-2} under room temperature. The photoluminescence spectra were carried out 300–650 nm regions for bare and doped LAAN single crystal shown in Fig. 4. The protonation of amino groups to the carboxyl groups as large concentrate and it's located at 425 nm region. It was clearly evident that the PL emission intensity of pure LAAN was relatively high compared with doped LAAN crystals. The PL emission intensity was gradually reduced with the presence of dopants. Especially, a significant reduction of PL intensity was found in the Cu-doped LAAN single crystals. This could be due to the prevention of electron–hole pair

Table 2 Vibrational assignments of pure and doped LAAN crystals

Pure LAAN	Cu-doped LAAN	Zn-doped LAAN	Mg-doped LAAN	Vibrations
3430	3446	3441	3435	OH stretching
3090	3107	3088	3086	NH stretching
2112	2121	2108	2107	NH_3^+ and COOH group
1595	1614	1599	1590	COO^- vibration
1410	1424	1412	1409	C–O stretching
1235	1238	1232	1228	COOH stretching
955	959	945	947	NO_3^- group
857	862	841	855	NO_3^- group

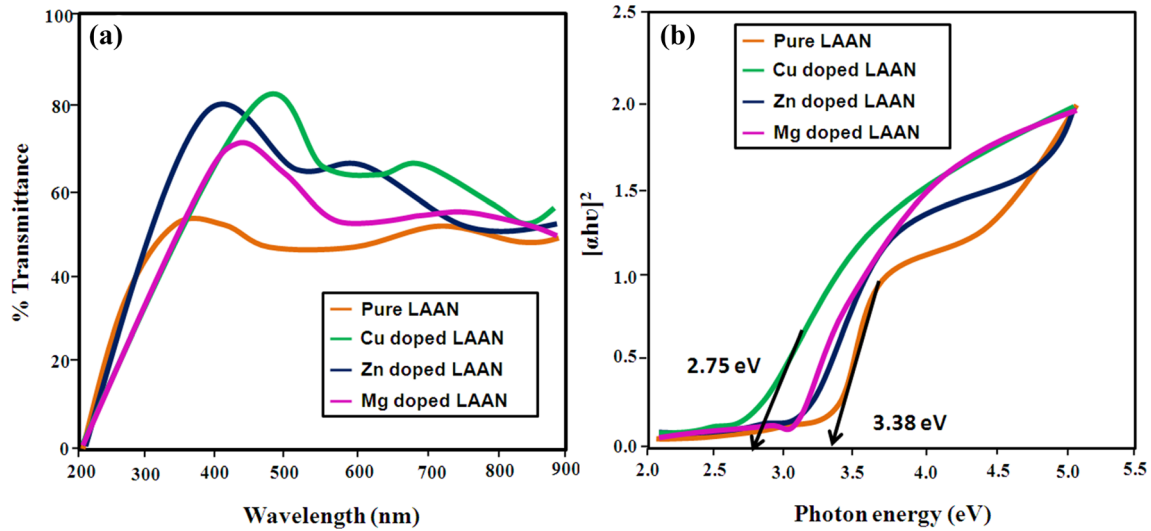


Fig. 3 a Transmittance spectra and b $(\alpha hv)^2$ vs photon energy plot of pure and doped LAAN crystals

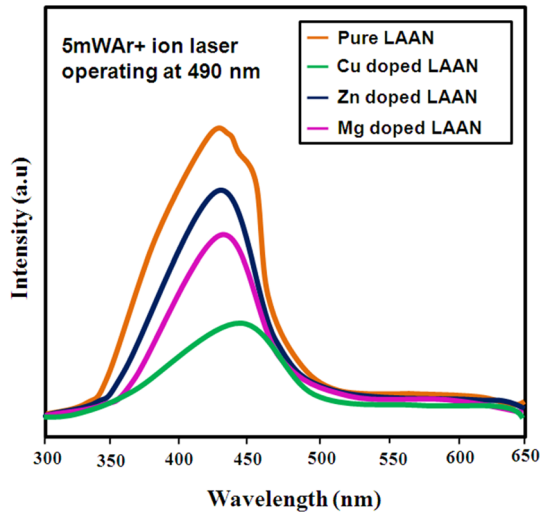


Fig. 4 Photoluminescence spectra of pure and doped LAAN crystals

recombination process. Hence the UV and PL results suggest that Cu-doped LAAN could effectively improve the absorption property and suppress the recombination process of electron–hole pair, which is positive role to significantly improve the SHG efficiency.

3.5 Microhardness studies

The Microhardness studies were carried by bare and doped LAAN single crystals. Fig. 5 shows the graph of microhardness studies plotted at various loads versus hardness number. The equation of $Hv = 1.8544 \times (p/d^2)$ was used to calculate hardness

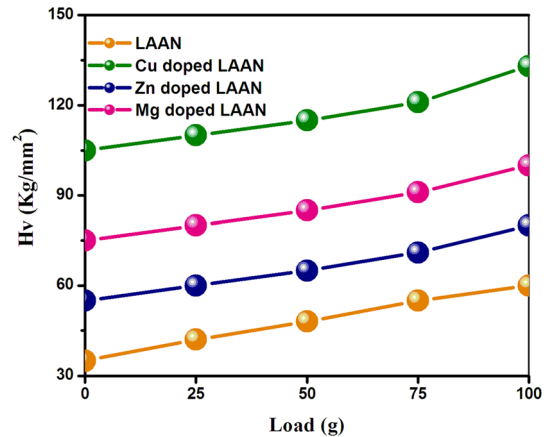


Fig. 5 Vickers hardness vs load of pure and doped LAAN crystals

numbers of growth crystals [26–28]. The expansion of above equation followed as Hv is the Vickers hardness number, p is the applied load, and d is the average diagonal length of the indentation mark. The Indentation size effect (ISE) was reversed for increasing the load and its clearly seen in graph plot [29]. Above the reasons to Cu-doped LAAN, single gem has located at tall hardness esteem compared to other gems. In this tall tackle esteem of the Cu-doped LAAN, precious stone esteem demonstrates more prominent push required to create separation, hence affirming more noteworthy crystalline flawlessness.

3.6 Dielectric studies

A rectangular specimen of pure and doped LAAN crystals was subjected to dielectric studies. Both

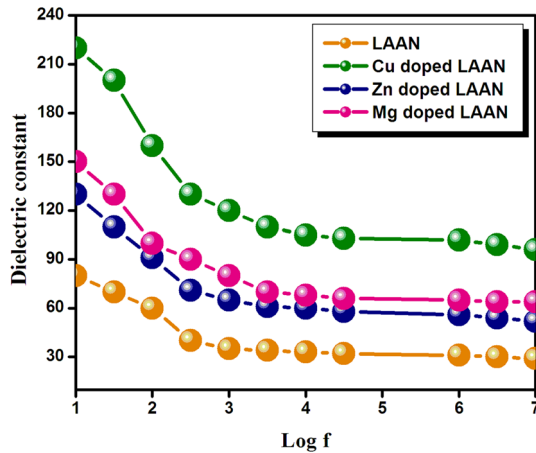


Fig. 6 Dielectric constant vs log frequency measured at 40 °C of pure and doped LAAN crystals

surfaces of the samples were coated with silver paste to make contact between the crystal and the copper electrodes. Figure 6 shows the plots of dielectric constant versus frequency for pure and doped LAAN crystals. It can be observed that as the frequency increases the dielectric constant decreases and for high-frequency region it remains almost constant for pure and doped LAAN crystals. This can be explained on the basis of polarization. The electronic exchange of the number of ions in the crystals gives local displacement of electrons in the direction of the applied field, which in turn is expected to give rise to the polarization. As the frequency of the applied field increases, a point will be reached where the space charge polarization cannot sustain and complies with variation of the external field and hence the polarization decreases. The dielectric constant and dielectric loss values were as calculated by previous published work [30]. Figure 7 shows the variation in dielectric loss with frequency for pure and doped crystals. From this figure, it can be seen that the dielectric loss decreases as the frequency increases for all samples. It can also be seen that, the dielectric loss is higher at lower frequencies for doping crystals when compared to the pure crystal. The characteristic of low dielectric loss with high frequency for a given sample shows that the sample possess good optical quality with lesser defects and this parameter is of vital importance for nonlinear optical materials in their application.

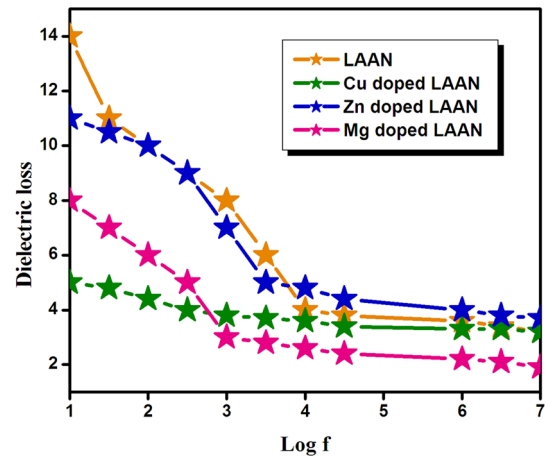


Fig. 7 Dielectric loss vs log frequency measured at 40 °C of pure and doped LAAN crystals

3.7 AC conductivity and photoconductivity studies

Fig. 8 shows the conductivity behavior of bare and metal-doped LAAN single crystal and this experiment of electrical conductivity conducted by temperature range between 30 and 90 °C. From Fig. 8a) it can be seen that the AC conductivity for all the samples increase with increase in temperature and the AC conductivity was found to increase after doping at all temperatures. The AC conductivity values for pure and doped crystals measured at room temperature with fixed frequency at 1 kHz. The defect concentration will increase exponentially with temperature and consequently the electrical conduction also increases. The measurements show that the Cu-doped LAAN crystals have larger conductivity than pure LAAN crystals. Under room temperature the electric conductivity delivers as 1.4, 5.2, 2.3, and 3.2 Ωm^{-1} for bare LAAN, Cu-, Zn-, Mg-doped LAAN single crystal, respectively, as shown in Fig. 8a. The Arrhenius relation used to found the activation energy by plot of $1000/T$ versus log conductivity [25]. Fig. 8b shows activation energies calculated by slope of $1000/T$ versus $\ln \sigma$ plot. From Table 3, it can be seen that the activation energy was found to decrease after doping. When LAAN crystals were doped with the impurities, the lattice defects increases and this enhances the conductivity and hence there is decrease in activation energy. Keithley 485 picoammeter and resultant without the light used to analyze the photoconductivity calculations for Cu-doped LAAN single crystal and the dim current was

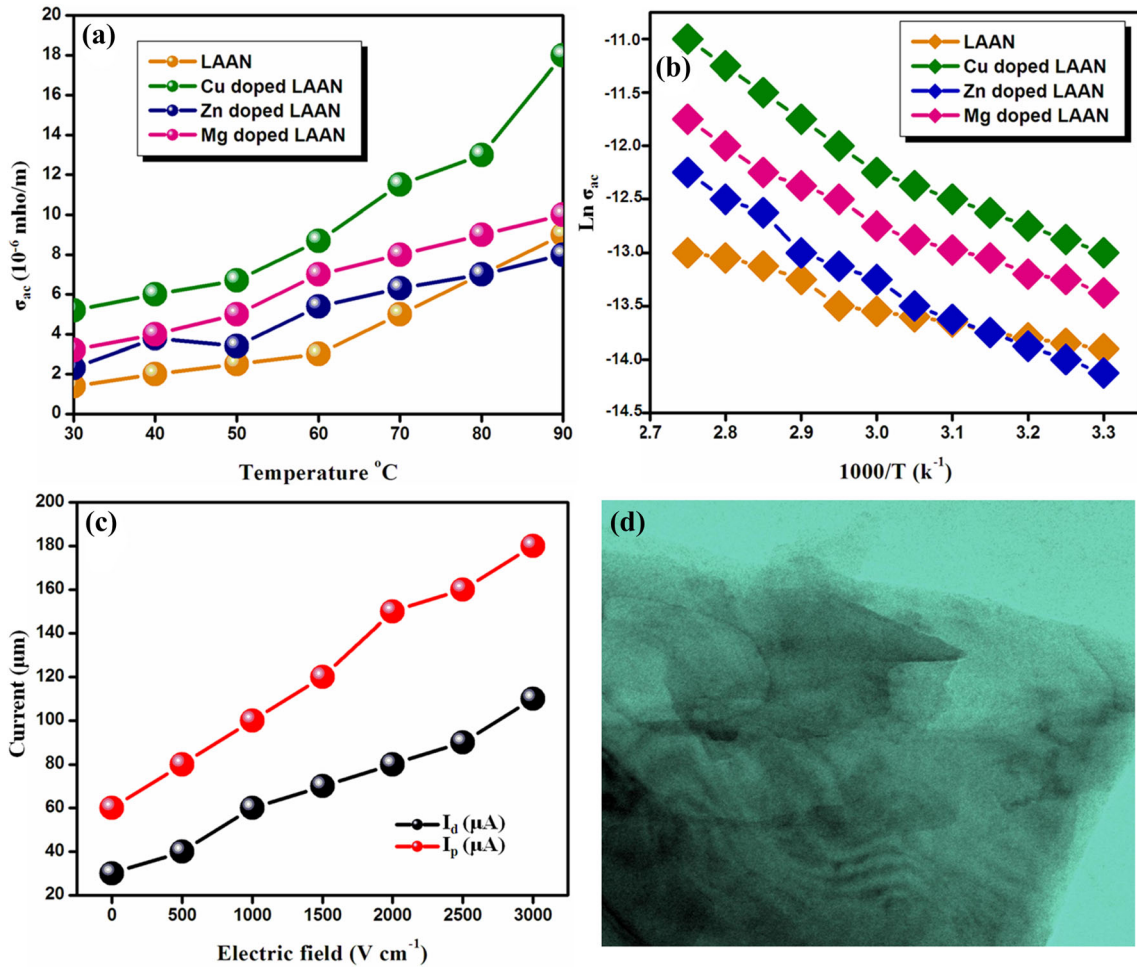


Fig. 8 **a** AC electrical conductivity versus temperature for pure and doped LAAN crystals; **b** variation of $\ln(\sigma)$ with $1000/T$ of pure and doped LAAN crystals; **c** field-dependent photoconductivity of Cu-doped LAAN; **d** etching photograph of Cu-doped LAAN

Table 3 AC conductivity and activation energy values of the pure and doped LAAN crystals

Crystals	AC conductivity (Ωm) ⁻¹	Activation energy (eV)
Pure LAAN	1.4	0.55
Cu-doped LAAN	5.2	0.21
Zn-doped LAAN	2.3	0.38
Mg-doped LAAN	3.2	0.27

measured for all the growth crystals. In Fig. 8c) shows the variety of both dull current (I_d) and photocurrent (I_p) with the connected electrical field. The Plot clearly shows connect to the electric field and I_d and I_p current test straightly increased. The plot above plot denotes dim current is continuously important than the photocurrent, and its confirm presence of negative photoconductivity. The etching studies were carried out on the grown crystal (Cu-doped LAAN) using Carl Zeiss High resolution optical microscope. Ethanol, methanol and water

were used as etchants. The photographs were taken with a maximum etching time of 60 s. The etch pattern of Cu-doped LAAN is shown in Fig. 8d). It is observed that etch pits are formed to the etching time of 60 s. A number of carve pits have been recognized with indistinguishable shape. By expanding the carving time, the design remains the same, but the measure of the carve pits has expanded. It is observed that the less number of disengagements appears the quality of the crystal.

3.8 SHG efficiency test

The SHG conversion efficiency of pure and doped LAAN crystals was estimated using modified setup of Kurtz and Perry. A Q-switched Nd:YAG laser beam of wavelength 1064 nm was used with an input power of 2.15 mJ and pulses width 10 ns with a repetition rate of 10 Hz. The crystals were powdered and then packed in a micro-capillary of uniform bore and exposed to laser radiations. The output from each sample was monochromated (monochromator, model Triax, 550) to collect the intensity of 532 nm component. The second harmonic radiation generated by the randomly oriented microcrystals was focused by a lens and the green light was detected by a photomultiplier tube (PMT, Philips Photonics, model 8563) and displayed on a cathode ray oscilloscope (CRO) (Tektronix-TDS 3052B). A green radiation of 532 nm was observed from the pure and doped LAAN crystals confirming the second harmonic generation (SHG). The efficiency of bare and doped LAAN crystal is better than standard efficiency of KDP. The SHG efficiency of bare and doped (Cu, Zn and Mg) LAAN crystals values are 2.1, 3.2, 1.5, and 1.8 times, respectively (Fig. 9). In the result, Cu-doped LAAN single crystal has 3.2 times large efficiency for other growth crystals. The improved SHG may be concluded that the protonation of the amino group in the L-alanine molecule is the key factor in increasing the relative SHG efficiency of LAAN. SHG output enhances considerably with the Cu doping which is one of the most important findings of the present investigation. Moreover, the metallic nature of Cu could provide higher electrical

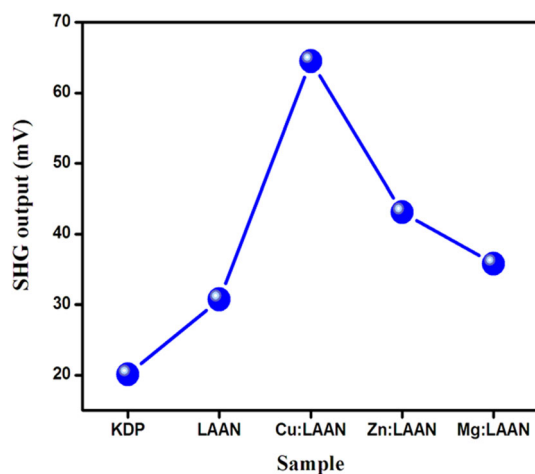


Fig. 9 SHG efficiency of pure and doped LAAN crystals

nature of pure LAAN. In addition, the optical absorption is significantly improved in the visible light region and the band gap energy by Cu doping is narrowed compared with other dopants and pure LAAN. The effective prevention of the recombination process of electron–hole pair is another crucial factor to improve the SHG efficiency. The overall results suggest that Cu-doped LAAN crystals show high optical, mechanical, dielectric electrical, and NLO properties.

4 Conclusions

The single crystals of pure LAAN and doped with Cu, Zn, and Mg were grown by slow evaporation technique at room temperature. Single crystal X-ray diffraction analysis was carried out to calculate the lattice parameters of the grown crystals. The lattice parameter of both crystals like $a = 7.851 \text{ \AA}$, $b = 5.441 \text{ \AA}$, $c = 12.806 \text{ \AA}$, $\beta = 94.75^\circ$, and volume of $V = 547 \text{ \AA}^3$ belong to space group P21. The FTIR results are used to confirm formation of LAAN single crystal. Especially, Cu-doped LAAN crystal UV–Vis spectrum of red shift was absorbed at $\sim 450 \text{ nm}$. The transparency of single crystals of bare and doped LAAN crystal exhibited 55–60% and 80–90%, respectively. The good transmission property of the pure and doped LAAN crystal in the entire visible region ensures its suitability for SHG applications. A significant prevention in the electron–hole recombination process of PL emission is another key factor to improve the SHG. The low value of dielectric constant and dielectric loss at higher frequencies suggests that the crystals possess enhanced optical quality which has significant role in the NLO applications. The AC conductivity result reveals that the electric conductivity delivers as 1.4, 5.2, 2.3, and $3.2 \text{ \Omega m}^{-1}$ for pure and Cu-, Zn-, Mg-doped LAAN single crystal, respectively.

References

1. M. Meena, C.K. Mahadevan, Growth and electrical characterization of larginine added KDP and ADP single crystals. *Cryst. Res. Technol.* **43**, 166–172 (2008)
2. P.S. Ramasubramanian, C. Mahadevan, Growth kinetics and electrical properties of KCl doped single crystals grown from

- aqueous solutions. *Indian J. Pure Appl. Phys.* **29**, 285–287 (1991)
3. T. Chithambarathanu, C. Mahadevan, T. Josephine Rani, Refraction equivalent measurements on K_2CrO_4 and $K_3Fe(CN)_6$ doped KDP single crystals. *J. Opt.* **22**, 21–22 (1993)
 4. K. Sangwal, E. Mielniczek-Brzowska, Effect of impurities on metastable zone width for the growth of ammonium oxalate monohydrate crystals from aqueous solutions. *J. Cryst. Growth* **267**, 662–675 (2004)
 5. E. Mielniczek-Brzowska, K. Sangwal, Growth kinetics of ammonium oxalate monohydrate single crystals from aqueous solutions containing Co(II) and Ni(II) impurities. *Cryst. Res. Technol.* **39**, 993–1005 (2004)
 6. S. Karan, S.P. Sen Gupta, Microhardness studies on urea-doped solution growth single crystals of epsomite. *Indian J. Phys.* **80**, 781–787 (2006)
 7. C.K. Mahadevan, R.S.S. Saravanan, Nucleation parameters of pure and impurity added $MgSO_4 \cdot 7H_2O$ single crystals. *Mater. Manuf. Process.* **22**, 357–361 (2007)
 8. K. Vasantha, P.A. Angeli Mary, S. Dhanuskodi, EPR and optical absorption studies of VO (II) doped zinc tris thiourea sulfate. *Spectrochim. Acta A* **58**, 311–316 (2002)
 9. S. Meenakshisundaram, S. Parthiban, N. Sarathi, R. Kalavathy, G. Bhagavannarayana, Effect of organic dopants on ZTS single crystals. *J. Cryst. Growth* **293**, 376–381 (2006)
 10. A. Anne Assencia, C. Mahadevan, DC electrical conductivity measurements on ADP single crystals added with simple organic compounds. *Bull. Mater. Sci.* **28**, 415–418 (2005)
 11. R. Ananda Kumari, R. Chandramani, Second harmonic generation efficiency in KDP crystals containing alkali halides. *Indian J. Phys.* **77A**, 397–399 (2003)
 12. G. Deepa, T.H. Freeda, C. Mahadevan, DC electrical conductivity measurements on KDP single crystals added with NaCl and NaBr. *Indian J. Phys.* **76A**, 369–372 (2002)
 13. C.K. Mahadevan, DC electrical conductivity measurements on KCl and KNO_3^- added $MgSO_4 \cdot 7H_2O$ single crystals. *Phys. B* **403**, 57–60 (2008)
 14. M. Lydia Caroline, S. Vasudevan, Growth and characterization of an organic nonlinear optical material: l-alanine alaninium nitrate. *Mater. Lett.* **62**, 2245–2248 (2008)
 15. A. Aravindan, P. Srinivasan, N. Vijayan, R. Gopalakrishnan, P. Ramasamy, A comparative study on the growth and characterization of nonlinear optical amino acid crystals: l-alanine (LA) and l-alanine alaninium nitrate (LAAN). *Spectrochim. Acta A* **71**, 297–304 (2008)
 16. M. Vimalan, X. Helan Flora, S. Tamilselvan, R. Jeyasekaran, P. Sagayaraj, C.K. Mahadevan, Optical, thermal, mechanical, and electrical properties of a new NLO material: mono-l-alaninium nitrate (MAN). *Arch. Phys. Res.* **1**(3), 44–53 (2010)
 17. R. Gopalakrishnan, P. Ramasamy, Reply to “comments on papers reporting IR spectra and other data of l-alanine alaninium nitrate and l-alanine sodium nitrate crystals” by M. Fleck and A. M. Petrosyan. *Cryst. Res. Technol.* **44**(7), 773–775 (2009)
 18. A. Aravindan, P. Srinivasan, N. Vijayan, R. Gopalakrishnan, P. Ramasamy, Investigations on the growth, optical behaviour and factor group of an NLO crystal: l-alanine alaninium nitrate. *Cryst. Res. Technol.* **42**(11), 1097–1103 (2007)
 19. G.G. Muley, M.N. Rode, B.H. Pawar, FT-IR, thermal and NLO studies on amino acid (l-arginine and l-alanine) doped KDP crystals. *Acta Phys. Pol. A* **116**(6), 1033–1037 (2009)
 20. M. Ramos Silva, J.A. Paixão, A. Matos Beja, L. Alte da Veiga, Strong hydrogen-bonded amino acid dimers in l-alanine alaninium nitrate. *Acta Crystallogr. C* **57**, 838–840 (2001)
 21. J.G. Arul Raj, P. Selvarajan, S. Perumal, N. Murali Krishnan, Investigations on growth and characterization of undoped and thiourea-doped γ -glycine crystals for NLO applications. *Mater. Manuf. Process.* **26**, 1254–1260 (2011)
 22. R. Sudha Periathai, K. Rajagopal, FTIR and Raman vibrational investigations on the complex of pyridine with tartaric acid. *IOSR J. Appl. Phys.* **6**, 9–12 (2014)
 23. J. Tauc, *Amorphous and Liquid Semiconductors* (Springer, New York, 1974).
 24. R. Uthrakumar, C. Vesta, C. Justin Raj, S. Krishnan, S. Jerome Das, Bulk crystal growth and characterization of nonlinear optical bithiourea zinc chloride single crystal by unidirectional growth method. *Curr. Appl. Phys.* **10**, 548–552 (2010)
 25. R. Parimaladevi, C. Sekar, V. Krishnakumar, The effect of nitric acid (HNO_3) on growth, spectral, thermal and dielectric properties of triglycine sulphate (TGS) crystal. *Spectrochim. Acta A* **75**, 617 (2010)
 26. N. Pattanaboonmee, P. Ramasamy, P. Manyum, Optical, thermal, dielectric and mechanical studies on glycine doped potassium dihydrogen orthophosphate single crystals grown by SR method. *Proced. Eng.* **32**, 1019–1025 (2012)
 27. K. Sangwal, Review: indentation size effect, indentation cracks and microhardness measurement of brittle crystalline solids—some basic concepts and trends. *Cryst. Res. Technol.* **44**, 1019–1037 (2009)
 28. V. Chithambaram, S. Jerome Das, R. Arivudai Nambi, K. Srinivasan, S. Krishnan, Effect of metallic dopants on potassium acid phthalate (KAP) single crystals. *Phys. B* **405**, 2605–2608 (2010)
 29. P. Selvarajan, J. Glorium Arulraj, S. Perumal, Structural, mechanical, optical, dielectric and SHG studies of undoped and urea-doped γ -glycine crystals. *Phys. B* **405**, 738–743 (2010)

30. K. Pandurangan, S. Suresh, Synthesis, growth, and characterization of bisglycine hydrobromide single crystal. *J. Mater.* (2014). <https://doi.org/10.1155/2014/362678>

Publisher's Note Springer Nature remains neutral with regard to jurisdictional claims in published maps and institutional affiliations.